Available online at www.sciencedirect.com
SCIENCE DIRECT
Journal of Photochemistry and Photobiology A: Chemistry 181 (2006) 274–282
Journal of Photochemistry and Photobiology A:Chemistry
www.elsevier.com/locate/jphotochem

Gradual change of one- and two-photon absorption properties in solution—Protonation of 4-*N*,*N*-dimethylamino-4′-aminoazobenzene

Liudmil Antonov [a,b,*], Kenji Kamada [a,**], Daniela Nedeltcheva [c], Koji Ohta [a], Fadhil S. Kamounah [d]

[a] *Photonics Research Institute, National Institute of Advanced Industrial Science and Technology (AIST), Ikeda, Osaka 563-8577, Japan*
[b] *Department of Chemistry and Biochemistry, National Forestry University, 10 Kliment Ohridski Avenue, Sofia 1756, Bulgaria*
[c] *Institute of Organic Chemistry, Bulgarian Academy of Sciences, Akad. G.Bonchev Street, bl.9, Sofia 1113, Bulgaria*
[d] *CISMI, Department of Chemistry, University of Copenhagen, Universitetsparken 5, DK-2100 Copenhagen, Denmark*

Received 6 April 2005; received in revised form 1 July 2005; accepted 5 July 2005
Available online 25 January 2006

Abstract

Linear (one-photon) and nonlinear (two-photon) spectral properties of 4-*N*,*N*-dimethylamino-4′-aminoazobenzene have been investigated under protonation in DMSO/water solvent mixtures. Observed spectral changes have been discussed in terms of ammonium–azonium tautomerism. The corresponding tautomeric constants have been determined for the first time for such kind of tautomeric equilibria. The process of protonation leads to changes of the two-photon absorption properties, suggesting that such process could be used as a tool for change of third-order nonlinear optical activity in solution.

Keywords: Aminoazobenzenes; Protonation; Ammonium–azonium tautomersim; Two-photon absorption; Femtosecond Z-scan technique

1. Introduction

It is well known that azobenzenes containing amino or dialkylamino groups undergo a pronounced color change in solution or in polymer film under protonation [1,2]. This phenomenon, caused by redistribution of the electronic density in protonated dye molecules and called halochromism, lies in the basis of their use as optical sensors [3,4].

The relative effect of the color changes in such dyes is associated with the existing ammonium–azonium tautomerism [5,6] and with the tautomeric ratio, which depends, as usual, on the solvent, temperature, irradiation and existence of additional substituents in the protonated molecule. However, it is in general very difficult to study such kind of tautomeric processes, because the individual responses of the pure tautomers are unknown. Recently we developed an approach for analysis of tautomeric equilibria [7–9], allowing to shed additional light on ammonium–azonium tautomerism, which is one of the aims of this study.

In this paper, we investigate the color changes of 4-*N*,*N*-dimethylamino-4′-aminoazobenzene (structure **A**, Scheme 1) under protonation in DMSO/water solvent mixtures. This compound, containing two donor groups and an π electronic bridge (azo group), is a typical D–π–D system and represents also an interest as nonlinear optical material [10]. Under protonation this system can be gradually transformed to A–π–D and finally to A–π–A, which gives a possibility for changes of the nonlinear optical properties keeping, however, the same origin of the molecule. Recently, we have shown by two-photon absorption (2PA) technique the importance of donor and acceptor strength on the third-order nonlinear properties of a series of A–π–D molecules containing stilbene, azo and azomethine fragments as π electronic bridge [11]. At the same time it has been reported that in the case of symmetrically and asymmetrically substituted stilbenes the systems D–π–D have higher two-photon absorption response than A–π–D [12].

Therefore, the aims of this study are: (1) to investigate the process of protonation of **A** by linear (one-photon) absorption

* Corresponding author. Tel.: +359 2 91907.
** Corresponding author.
E-mail addresses: lantonov@orgchm.bas.bg (L. Antonov), k.kamada@aist.go.jp (K. Kamada).
URL: http://www.orgchm.bas.bg/∼lantonov.

1010-6030/$ – see front matter © 2005 Elsevier B.V. All rights reserved.
doi:10.1016/j.jphotochem.2005.07.025

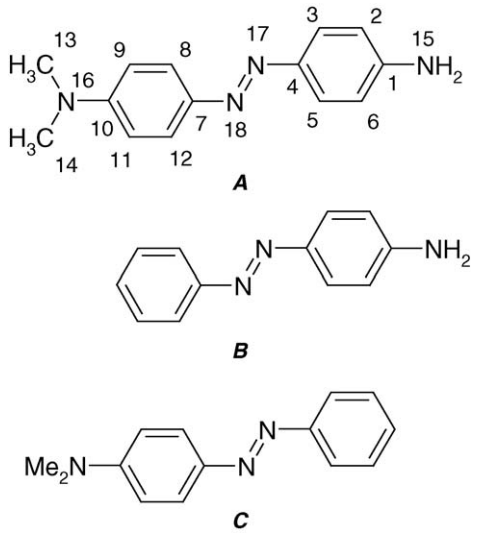

Scheme 1.

spectroscopy, estimating the individual responses of the tautomeric forms and the tautomeric ratios; (2) to understand how the change of the molecular structure under protonation would affect the third-order nonlinearity and whether the protonation of such dyes is suitable as a tool for gradual switching of their nonlinear optical properties. Although in this case the results are more of theoretical interest, in our best knowledge there are no studies to shed light on the changes of 2PA under protonation.

2. Experimental part

2.1. Materials

All compounds used in this study were synthesized by standard procedures and then purified by column chromatography. Spectral grade (Kanto Chemical Co., Inc.) dimethyl sulfoxide (DMSO) was used as solvent for the optical measurements. Protonation experiments[1] were performed by using 1N standard solution of HCl (Kanto Chemical Co., Inc.). Sets of solutions with both 10% and 30% water content,[2] keeping dye concentration constant, but varying amounts of HCl, were prepared using a stock dye solution in DMSO.

2.2. Linear absorption measurements

The UV–vis (one-photon) absorption spectra of the solutions with dye concentrations in the range up to 5×10^{-5} M were recorded by a Shimadzu UV-3150 UV–Vis–NIR spectrophotometer in a 1 cm quartz cell. The obtained spectral curves under protonation were processed by using the previously described "fishing-net" algorithm [7,8] and the software MULTIRES [9]. As a result, the individual spectra of mono- and biprotonated forms were estimated along with the molar fractions of neutral and protonated species. The error of estimation is within 2% [8,9].

2.3. Two-photon absorption experiments

Third-order nonlinear optical properties of the sample solutions were measured by the Z-scan technique [13]. The optical setup is illustrated in details elsewhere [11,14]. It includes an optical parametric amplifier (Spectra-Physics OPA-800), pumped by Ti:sapphire regenerative amplifier system (Spectra-Physics Spitfire, Tsunami and Millennia) operating at the repetition rate of 1 kHz, used as light source. The output pulse width was 100–130 fs. The dye concentrations of the sample solutions were adjusted so that the open apertures Z-scan signals to be detected (10 mM) in a 1 mm quartz cell. In general **A** is very well soluble in DMSO, but its solubility decreases with increasing amount of water and the used concentration of 10 mM is the highest possible concentration in 30% water content. The sample solutions in these high concentrations were sandwiched between fused quartz plates and their UV–vis spectra were measured. The recorded one-photon spectra of the solution films did not differ as shape from those in diluted solutions, showing the lack of concentration dependent phenomena (self-association). During the Z-scan experiments the stability of each sample was confirmed by measuring of UV–vis absorption before and after each experiment. The obtained Z-scan data were processed as described previously [11] by using of global fitting procedure [15] and then the corresponding 2PA cross sections $\sigma^{(2)}$ were estimated.[3] The measured Z-scan signals at definite wavelength were linear to the source power (0.1–0.6 mW), proving a pure 2PA process [11,14].

2.4. Quantum-chemical calculations

All calculations were done with the Gaussian 98 program suite [16] at the Hartree–Fock (HF) 6-31G** level of theory. All optimized structures were characterized as true minima by vibrational frequency calculations. Bulk solvent effects in DMSO and water were estimated by single-point calculations using the polarized continuum model (PCM) [17,18].

3. Results and discussion

3.1. Linear spectral properties under protonation

The spectral changes of **A** in solution under protonation are shown in Fig. 1. These changes are result of the existing ammonium–azonium tautomerism as given in Scheme 2. As seen, depending on the position of protonation (NH_2 or NMe_2) two possible equilibria exist in the monoprotonated stage. In Fig. 1a decrease of the band of the neutral form (around

[1] The pH values used in the paper are the apparent pH values, calculated as free HCl in the solution after estimation of the protonated species content.

[2] In this paper the DMSO/water solvent compositions are defined as water content given in volume percents.

[3] In this paper the values of $\sigma^{(2)}$ are reported in GM units. $1\,\mathrm{GM} = 1 \times 10^{-50}\,\mathrm{cm^4\,s\,photon^{-1}\,molecule^{-1}}$.

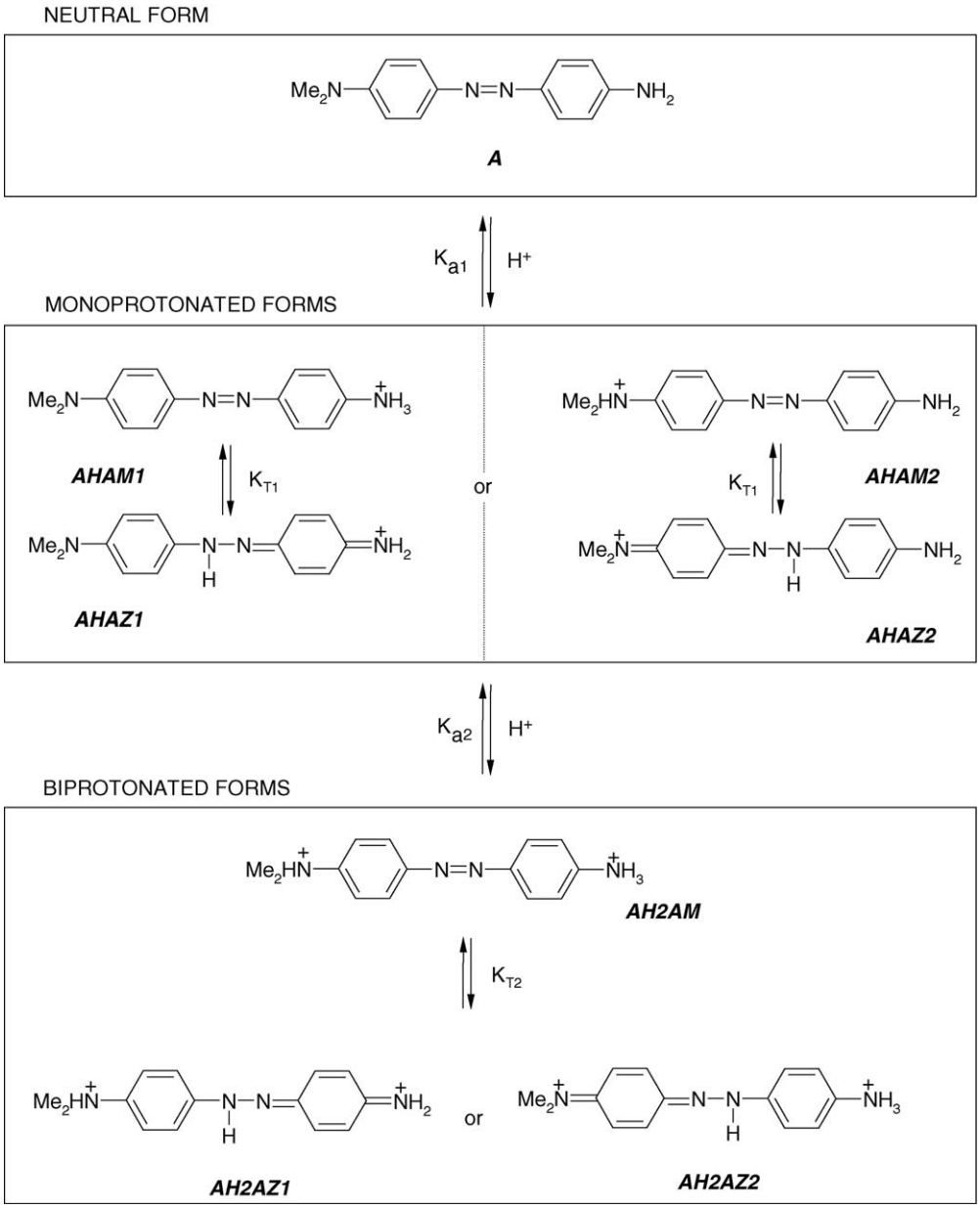

Scheme 2.

450 nm) is observed after addition of acid,[4] giving rise of new band at 620 nm assigned to the azonium form (**AHAZ**). Obvious spectral evidences for appearance of the ammonium form (**AHAM**) are not observed. In the **AHAM** structure the amino (or dimethylamino) group is protonated and practically excluded from the conjugation with the rest of molecule. Therefore, its spectrum could be very similar to those of **B** (for **AHAM2**) or **C** (for **AHAM1**), strongly overlapped with the band of the neutral band and visually undetecteable. Further addition of HCl leads in 30% water (Fig. 1a) to decrease of **AHAZ** band and to appearance and rise of new band at 520 nm, belonging to biprotonated ammonium–azonium form **AH2AZ**. Similar rise attributed to the biammonium form **AH2AM** is observed at 300–320 nm, which corresponds to the absorption maximum of the azobenzene.

It is evident from the spectra shown in Fig. 1a that the second protonation begins before the first protonation to be finished and the mono- and biprotonated forms co-exist. Therefore, the individual spectra of mono- and biprotonated forms cannot be experimentally measured and the quantitative analysis of these processes is impossible in terms of classical spectrophotometry. However, these spectra have been processed by using the advanced chemometric procedure "fishing-net algorithm" [7–9]

[4] It is worth noting that in 10% water first addition of small amount of acid leads not to protonation, but to increase of the intensity of the band belonging to neutral form (Fig. 1b). Obviously this first portion of HCl (H_3O^+) causes destruction of the DMSO shell and establishes the new solvation equilibrium after addition of water as shown in Appendix A.

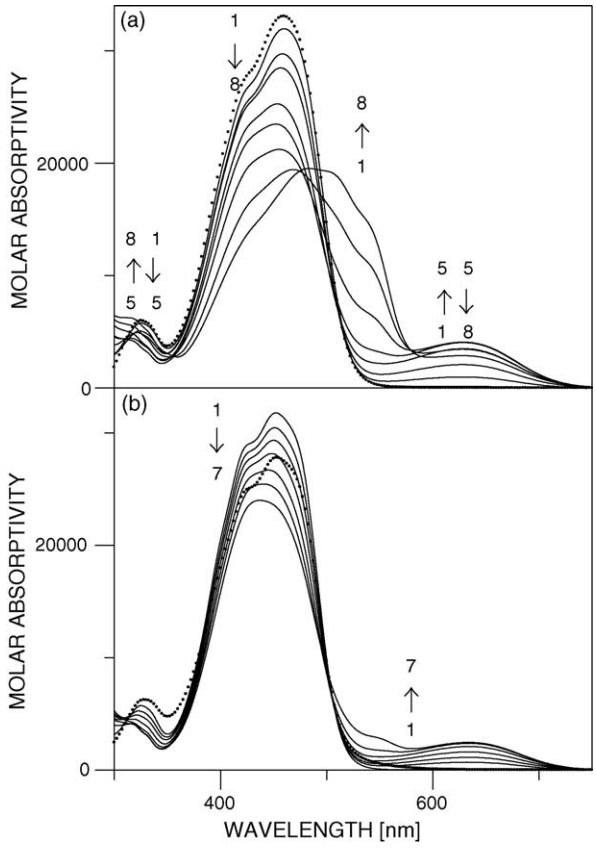

Fig. 1. Absorption spectra of **A** under protonation: (a) in 30% water, pH units—1: 3.70; 2: 2.52; 3: 2.22; 4: 1.70; 5: 1.40; 6: 1.00; 7: 0.70; 8: 0.52; (b) in 10% water, pH units—1: 3.80; 2: 2.50; 3: 2.20; 4: 1.90; 5: 1.60; 6: 1.30; 7: 1.00. The spectra without addition of acid are given in dots.

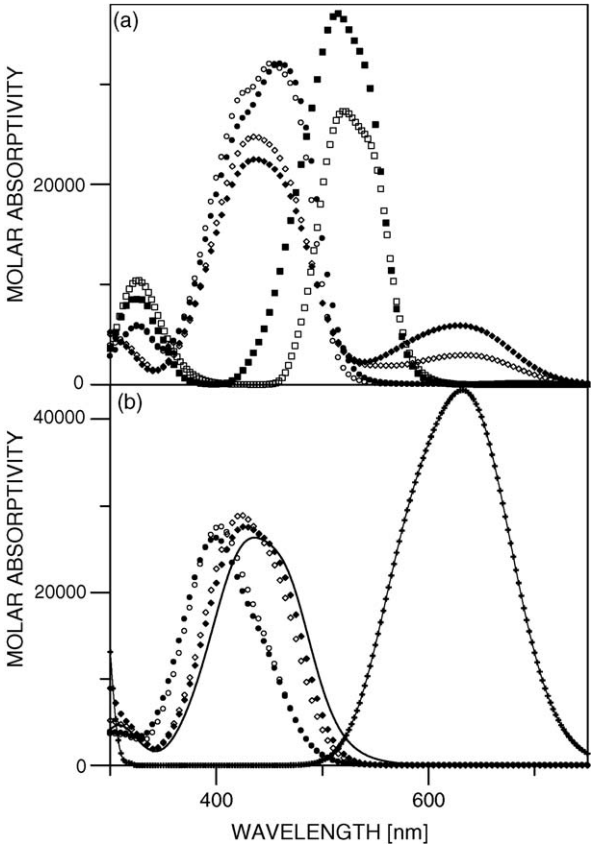

Fig. 2. (a) Estimated spectra of neutral (circles), mono- (rhombs) and biprotonated (squares) forms in 10% water (empty characters) and in 30% water (filled characters); (b) absorption spectra of **B** (circles) and **C** (rhombs) in 10% water (empty characters) and in 30% water (filled characters). Estimated absorption spectra of ammonium form (line) and azonium form (cross line).

and the corresponding spectral curves of the neutral, mono- and biprotonated forms, in both 10% and 30% water, have been estimated (Fig. 2a).

According to Fig. 2a, the absorption spectra of the neutral form in 10% and in 30% water are almost with the same intensity, but the redistribution of vibrational subbands, due to the solvent composition change,[5] is evident. As expected, in the case of monoprotonation, the absorption band at 430 nm belonging to ammonium form overlaps with the spectrum of the neutral form and therefore cannot be directly observed.

The most important results from Fig. 2a are that the fraction of the ammonium form dominates and decreases with increasing of water content. The opposite is observed for the azonium form. Similar process is observed in the case of biprotonation: the biammonium band at 320 nm decreases slightly, while the ammonium–azonium band at 520 nm increases with water content lift.

As a result of the chemometric procedure applied, the pK_a values have been also estimated (Table 1). Applying the same chemometric procedure on the curves representing the tautomeric mixtures in 10% and in 30% water (Fig. 2a) it was possible to estimate the corresponding tautomeric constants

Table 1
Estimated protonation and tautomeric constants[a]

Water (%)	K_{T1}	pK_{a1}	pK_{a1}^{AM}	pK_{a1}^{AZ}	K_{T2}	pK_{a2}
10	0.07	1.94 ± 0.04	1.91	0.78	0.53	–[b]
30	0.16	1.88 ± 0.04	1.81	1.01	0.88	0.37 ± 0.07

[a] K_T = [azonium]/[ammonium]; $pK_a^{AM} = pK_a - \log(1 + K_T)$, $pK_a^{AZ} = pK_a - \log(1 + 1/K_T)$.
[b] Very low, impossible to be determined.

(azonium/ammonium ratio, Table 1) as well as to calculate the individual spectra of the tautomers[6] (Fig. 2b). The curves given in Fig. 2 and the data collected in Table 1 are the first quantitative values ever reported for this kind of tautomeric equilibrium.

Availability of the individual spectrum of the ammonium form and its comparison with the spectra of the models **B** (for **AHAM2**) and **C** (for **AHAM1**) suggests a protonation at the NH_2 nitrogen. In other words the equilibrium ***AHAM1*** ⇄

[5] See Appendix A for more details.

[6] The estimated maximal intensities are as follows: $\varepsilon_{\mathbf{AHAM}} = 26{,}330$ at 436 nm; $\varepsilon_{\mathbf{AHAZ}} = 43{,}360$ at 632 nm; $\varepsilon_{\mathbf{AH2AZ}} = 79{,}160$ at 520 nm; $\varepsilon_{\mathbf{AH2AM}} = 16{,}130$ at 320 nm; the last value is in very good agreement with the reported $\varepsilon_{max} = 17{,}400$ (320 nm) for azobenzene in 96% ethanol [1] as well as with the measured by us value in DMSO ($\varepsilon_{max} = 16{,}700$ (322 nm)). All values for molar absorptivity are in l mol^{-1} cm^{-1} units.

Table 2
Calculated energies, atomic charges and bond lengths (HF/6-31G**)

Structure	E_{RHF} (a.u.)	Mulliken atomic charges (see Scheme 1 for atom numbering)				Bond length (Å)				
		N15	N16	N17	N18	N16–C10	C7–N18	N18–N17	N17–C4	C1–N15
A	−757.24010	−0.742	−0.706	−0.329	−0.330	1.386	1.414	1.222	1.415	1.389
AHAM1	−757.60556	−0.650	−0.731	−0.368	−0.292	1.359	1.389	1.230	1.411	1.483
AHAZ1	−757.63253	−0.752	−0.733	−0.198	−0.429	1.358	1.414	1.240	1.349	1.333
AHAM2	−757.62865	−0.756	−0.639	−0.292	−0.360	1.478	1.414	1.227	1.395	1.365
AHAZ2	−757.63424	−0.783	−0.716	−0.442	−0.202	1.332	1.340	1.244	1.417	1.356
AH2AM	−757.92130	−0.650	−0.646	−0.304	−0.300	1.476	1.422	1.218	1.423	1.482
AH2AZ1	−757.93369	−0.704	−0.647	−0.222	−0.531	1.475	1.404	1.287	1.293	1.305
AH2AZ2	−757.91659	−0.648	−0.681	−0.548	−0.247	1.301	1.284	1.300	1.396	1.480

AHAZ1 really exists in the case of monoprotonated form.[7] An additional proof in this respect is the fact that the pK_a values of **B** in 50% ethanol/water[8] is 2.07, while the corresponding value for **C** is 2.00 [5], suggesting easier protonation of NH_2 nitrogen.

The data from the quantum-chemical calculations, collected in Table 2, suggest a dominance of **AHAZ** forms in gas phase and a protonation at N16 (NMe_2) and N17 nitrogens.[9] These data are in contradiction with the experimental findings, but mark the importance of the specific interactions in the solution, which could stabilize additionally one or another form. At the same time the quantum-chemical results for the atomic charges and bong lengths describe well the structures given in Scheme 2. As seen from Table 2, the atomic charge at N15 (NH_2) in the case of **A** is higher than that at N16, which supports the experimentally proven protonation at NH_2 nitrogen. Such protonation decreases the π-electronic character of the Ph–N bond, without practically affecting the rest of molecule. As a result, the protonated aminogroup is practically excluded from the conjugated system, leading to spectral characteristics similar to those of **C**. In the case of azonium form a decrease of the double bond character of N–N along with increasing of π-electronic nature of N17–C4 and C1–N15 is observed. The data in Table 2 are consistent with the statistically evaluated experimental limits [20] for bond distances involved in azo linkage (1.37 Å < R(Ph–N=) < 1.49 Å; 1.20 Å < R(N=N) < 1.28 Å), showing that the azonium form mixes two mesomeric structures:

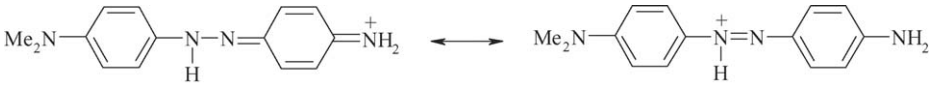

In general the dominance of **AHAM1** or **AHAZ1** depends on the electronic density at the corresponding N15 and N18 in the neutral form and one could find evidence in this respect comparing the pK_a AM and pK_a AZ values (Table 1). The values show that **AHAZ1** is stronger acid than **AHAM1**, which means that N15 is more basic than N18 in the neutral molecule and can be protonated more easily (of course the solvent can play an important role). At the same time **AHAZ1**, being stronger acid, can interact easier with proton acceptor solvents (like water), which could explain its stabilization with increase of water content. From structural point of view these conclusions are supported by the fact that azo group has acceptor nature and **AHAM1** is stabilized by donor substituents in the another phenyl ring (in our case it is NMe_2). In the case of azonium form the –NH– nitrogen could be considered as donor and preferred by acceptors, as shown by Gordon and Gregory [21].

From Table 1, one can conclude that in respect of biprotonated forms the content of ammonium–azonium form (**AH2AZ**) is substantial, but still not dominating. In this strongly conjugated structure an efficient charge transfer occurs behaving a value of molar absorptivity of almost 80,000 l mol^{-1} cm^{-1}. Again the ammonium–azonium form is more acidic than biammonium one (**AH2AM**), which determines its further stabilization in water.

3.2. Nonlinear absorption properties

The detailed information about the process of protonation and structure of the protonated tautomeric forms, obtained by linear spectroscopy, provides possibility to investigate protonation-related structural effects on the third-order nonlinearity of A.

As it was mentioned above, compound **A** represents a typical D–π–D system, which under protonation gradually changes to D–π–A (**AHAM1**) and then to A–π–A (**AH2AZ**). Such change allows to estimate the structural effects on the 2PA. Therefore,

[7] In general, the possible protonation site can be determined also by NMR spectroscopy. However, in this case, due to the fast proton exchange between the tautomeric forms and the unclear mechanism the performed ^{1}H NMR experiments have not provided clear picture about. Further experiments by ^{15}N NMR are planned to shed light on the mechanism of proton transfer at various temperatures.

[8] The values in ethanol/water and DMSO/water can be compared, because the same solvation model, based on specific interactions of water molecules with **A**, is assumed. The value of pK_a in DMSO/water is lower than in ethanol/water (2.15 [5]), which could be attributed to the better solvation of small positive ions (like H_3O^+) by DMSO [19].

[9] This contradiction can result from the strong dependence of the relative stability of tautomers, predicted by quantum chemistry, from the level of theory used in the calculations.

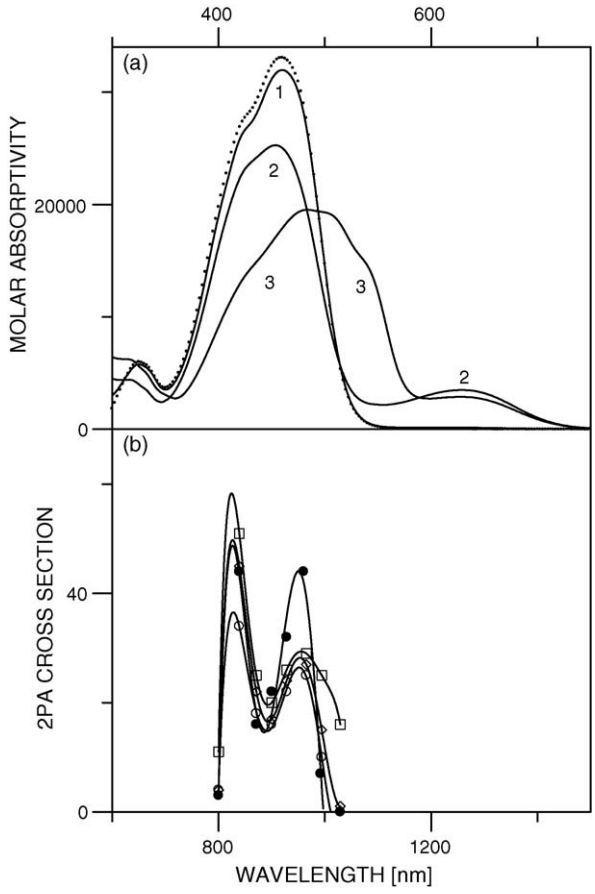

Fig. 3. Linear (a) and 2PA (b) spectra of **A** in 30% under protonation: (1) no acid added; (2) pH 1.90; (3) pH 0.52; dots—in DMSO only. In the 2PA spectrum the experimental points are given in empty characters as follows: (1) circles; (2) rhombs; (3) squares. The 2PA spectrum of **A** in DMSO is given in filled circles. The 2PA values are in GM units and the lines used are only for eye guide.

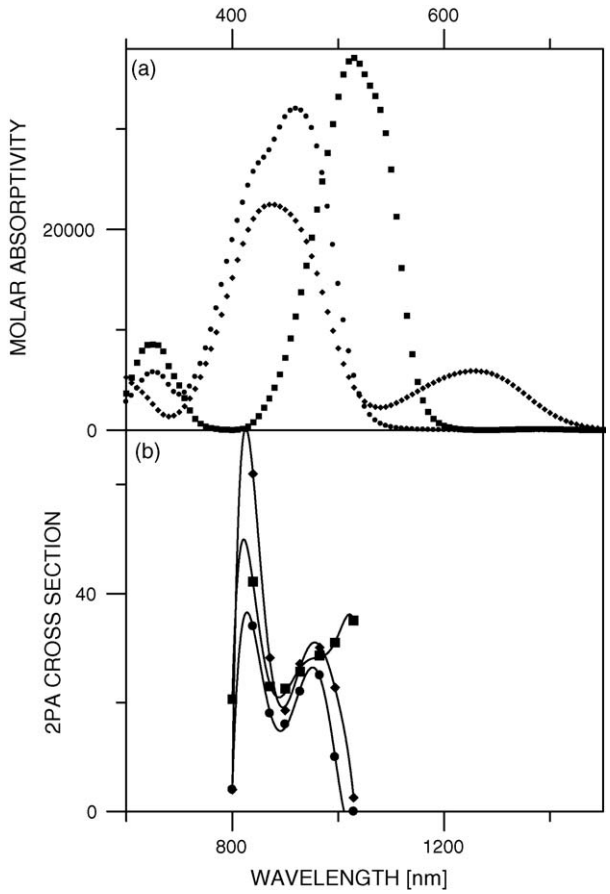

Fig. 4. Linear (a) and expected 2PA (b) individual spectra of neutral (circles), mono- (rhombs) and biprotonated (squares) forms of **A** in 30% water. The 2PA values are in GM units and the lines used are only for eye guide.

Z-scan experiments have been performed in DMSO/water solvent mixtures with 10% and 30% water content varying the acid content. The measured 2PA spectra under protonation are shown in Fig. 3. Two clear 2PA peaks are evident—sharp one at 839 nm and relatively broad one at 965 nm. Under protonation the intensity of the short-wavelength peak initially decreases in comparison with the pure DMSO and then sharply increases. Almost the same is the behavior of the peak at 965 nm, but the changes are less remarkable and no DMSO intensity is reached. The appearance of signal at 1030 nm, corresponding to biprotonated form, is evident. Of course these measured 2PA spectra represent a mixed signal originating from the existence of neutral and protonated species in each solution. At the same time it is possible to estimate the individual 2PA responses of protonated species, using the quantitative data available from the linear spectroscopy.

These individual 2PA curves are compared with the individual linear absorption spectra in Fig. 4. As discussed above, the neutral form exhibits two bands. Their positions correspond almost exactly to the vibrational subbands in the linear spectrum (422, 458 and 485 nm, determined by using of peak decomposition procedure) assigned by Mustroph [22] to vibronic transition from ground to excited state (0–0, 485 nm), N=N stretching vibronic transition (0–1, 458 nm) and torsional motion around the Ph–N(=) bond in the excited state (0–2, 422 nm). Therefore, it could be assumed that the 2PA spectrum of the neutral form has also vibrational structure. The 2PA curve of the monoprotonated form (**AHAM1**),[10] being already D–π–A system, remains with the same shape, but with increased intensity, concluding that the change from D–π–D (**A**) to D–π–A (**AHAM1**) leads to increase of the 2PA cross-sections. This finding is supported by the higher, than in **A**, 2PA cross-sections of D–π–A azobenzenes (for example, $\sigma^{(2)}$ = 178 GM at 973 nm for 4-nitro-4′-dimethylamino azobenzene) reported by us [11]. However, such a conclusion is in contradiction with the data reported by Wang et al. [12] for symmetric and asymmetric stilbene molecules. This contradiction suggests that general conclusions about the 2PA intensity structural effects valid for different classes of molecules could not be easily drawn.

In the case of biprotonated form (**AH2AZ**) a bathochromically shifted peak is detected[11] at 1030 nm, corresponding to

[10] Unfortunately, due to technical reasons, it has been impossible to measure the 2PA signals in the area 1050–1150 nm. After 1150 nm no signal for **AHAZ1** was detected, due to the low content of the azonium form and the insufficient intensity of its peak at 10 mM concentration.

[11] The linear absorption maximum of **AH2AM** is around 320 nm, which makes impossible its 2PA signal to be measured in the investigated mixtures.

Table 3
Estimated 2PA characteristics of the neutral and protonated species

Structure	Water (%)	2PA characteristics	
		λ_{max} (nm)	$\sigma^{(2)}$ (GM)
Neutral	0	839	44
		928sh	32
		960	44
	10	839	35
		928	28
		960sh	26
	30	839	34
		928sh	22
		960	25
Monoprotonated	10	839	65
		928	41
		960	34
	30	839	62
		928sh	27
		960	30
Biprotonated	10	1030[a]	56[a]
	30	839	42
		1030	35

[a] Due to the very low content of the biprotonated form it 2PA spectrum could be evaluated only at this wavelength.

the doubled position of the linear absorption band (520 nm). Surprisingly the sharp peak at 839 nm is also observed. It has been mentioned that this peak originates from Ph–N(=) torsion motion in excited state [22]. Such motion could be facilitated in the case of **AHAM1** (the decreased π-electronic character of the Ph–N(=) bonds)[12] leading also to increase of $\sigma^{(2)}$ in comparison with **A**, but could be forbidden in the linear spectrum of **AH2AZ**. Similar observation has been made in the 2PA spectrum of 4-nitro-4′-dimethylamino azobenzene [11], where an intensive and sharp short-wavelength peak appears without having origin in the linear spectrum. Another possibility of the sharp peak at 839 nm is interference between two transition dipole moments, which was reported for a similar molecule [23]. If there are two excited state located close to each other and transition dipole moments to the excited state have similar in magnitude but opposite sign, then one of 2PA transition was inhibited due to canceling out of the dipoles. In this case, the 2PA peak seems to be shifted and narrower compared to what are expected from the linear absorption peak for D–π–A molecules. Further detailed study is needed to clarify which process is the main contribution to the narrow 2PA band.

The available results for the 2PA intensity of **A** and its protonated species are collected in Table 3. These data allow an estimation of the effect of the medium to be performed. In the case of the neutral form the increase of the water content leads to gradual decrease of the 2PA cross sections. Such changes could be attributed to the H-bonding with the water molecules. The same effect is observed for the monoprotonated form from 10% to 30% water, but because at the same time a process of

[12] In the decomposed spectra of the neutral and monoprotonated form this subband has higher relative area in latter.

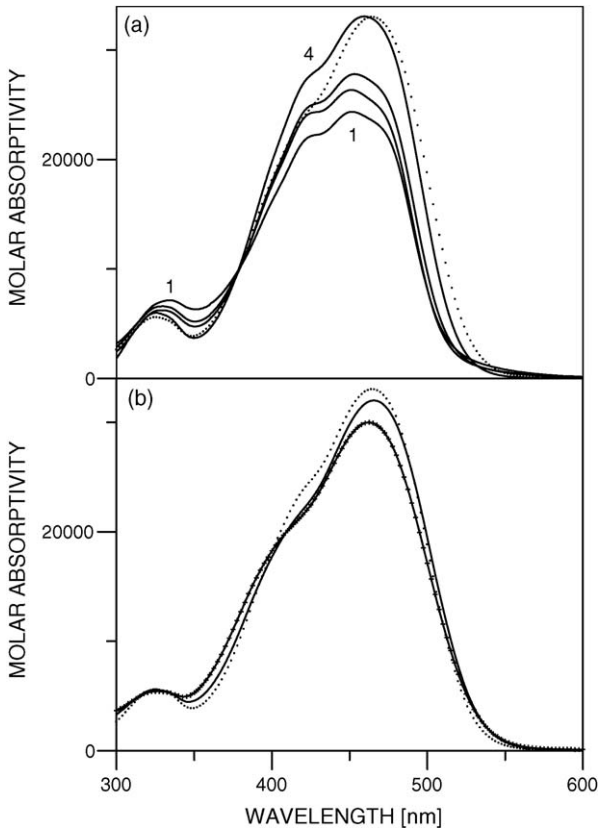

Fig. 5. Absorption spectra of **A** in various DMSO/water solvent mixtures as percentage of water—(a) 1: 0%; 2: 1%; 3: 10%; 4: 30%; dots: 50%; (b) filled dots: 50%; line: 70%; cross line: 90%.

stabilization of **AHAZ1** and decreasing of **AHAM1** is observed (according to the linear spectral results, Fig. 2a), it cannot be fully attributed as specific solvation effect. The changes in the 2PA spectra follow the changes in the individual linear spectra in Fig. 2a originating from the different ratio of the tautomers.

Acknowledgments

L.A. thanks Japanese Society for Promotion of Science (JSPS) for the provided fellowship at AIST and Alexander von Humboldt Foundation for the Return Fellowship.

Appendix A. Solvation of A in DMSO/water mixture

Absorption spectra of **A** in various DMSO/water mixtures are given in Fig. 5 and as seen exhibit an intensive vibronic band around 450 nm. Analyzing the curves as function of solvent composition, it would be concluded that the spectral behaviors in this case and the previously reported for ethanol/water mixtures (Figure 1 in [6]) differ considerably. In ethanol/water mixtures only redistribution of the intensity of the vibrational subbands, keeping the overall area of the composite peak almost constant, is observed. On the other hand, in the case of DMSO/water solvent composition initially a strong rise in the intensity is detected (from pure DMSO to 30% water, Fig. 5a), followed by a redistribution of the subbands' intensities (Fig. 5b).

Table 4
Calculated (PCM) solvation energies and dipole moments of **A**, **B** and **C** in DMSO

Compound	Gas phase		DMSO		$\Delta E_{solvation}$[a] (kcal/mol)	$\Delta G_{solvation}$ (kcal/mol)
	E_{RHF} (a.u.)	μ (D)	E_{RHF} (a.u.)	μ (D)		
A	−757.24010	0.971	−757.24897	1.017	5.57	−5.15
B	−624.15405	2.137	−624.16127	2.575	4.53	−3.69
C	−702.20528	2.586	−702.21083	3.056	3.48	−2.99

[a] As energy difference between gas phase and DMSO.

This behavior can be reasoned taking into account both the solute structures and the unique properties of the DMSO/water compositions.

According to Fabian and Hartmann [1], compound **A** can be described as a D–A–D system, where azo group plays role of acceptor. Such almost symmetric structure entails low dipole moment (Table 4), lack of acidic protons and increased electronic density at the nitrogen atoms. Consequently there are no possibilities for strong specific interactions with proton acceptor solvents like DMSO and same interactions with strong proton donor solvents could be expected.

DMSO as neat liquid solvent forms strong polymer-like clusters by interaction between its sulfur and oxygen atoms [24]. Its better solvation ability than water is reported in the case of aniline [19]. In case of lack of specific interactions, its solvation abilities are related to dispersion interactions with the aprotic (hydrophobic) moieties in the solute, which allows the PCM model solute–solvent interactions to be used [17,18]. The solvation energies from gas phase to DMSO as well as $\Delta G_{solvation}$ values, calculated by the PCM model, are given in Table 4. As seen, the solvation is much better in the case of nonpolar **A** than in the case of relatively polar **B** and **C**. Also taking into account the fact that **A** is soluble in DMSO as more as 50 mM, the solubility of **B** and **C** is lower and the solubility of 4-nitro-4′-dimethylamino azobenzene is around 1 mM, it could be concluded that the solvation shell around **A** molecules is much stronger than that in the case of **B** and **C**.

It is expected that the DMSO clusters could be destroyed in presence of proton donor solvents like water. However, in DMSO/water mixtures, as proven by neutron diffraction, ^{1}H NOESY NMR and mass spectrometry [25–27] as well as by molecular dynamics simulations [28,29], the structure of DMSO clusters is dominating in the solvent composition up to 70% water (molar fraction of water $X_w \leq 0.9$). At $X_w \leq 0.4$ (less than 15% water) 2DMSO/1H_2O and 1DMSO/1H_2O complexes exist; the behavior of mixtures with $0.4 \leq X_w \leq 0.6$ (approximately 15–30% water) is governed by 1DMSO/1H_2O and 1DMSO/2H_2O; and at $X_w \geq 0.6$ the presence of 1DMSO/2H_2O and higher number of water molecules [30] complexes is dominating. At $X_w \geq 0.9$ the water clusters (typical water structure) is observed.

These experimental facts match very well the picture observed in Fig. 5. In pure DMSO (Fig. 5a) a rigid solvation cage, based on nonspecific interactions,[13] is available around the solute molecule. After addition of water gradual processes of replacement of DMSO in the solvation shell occur leading to destruction the DMSO cage by forming DMSO/water complexes and solvation of **A** by establishment of H-bonding with the water molecules.

These two processes correspond to the curves of 1%, 10% and 30% water. Finally at 30% water we can consider that a new solvation equilibrium is established—a complex of **A** with water molecules caged by a mixed DMSO/water solvation shell[14]. After that, the further increase of water content (Fig. 5b) leads to changes in the solvation shell (bulk solvent effect) and to effect of intensity redistribution in the absorption spectra, similar to those observed in the case of ethanol/water mixtures. It is worth noting that in the case of ethanol/water the competition is between ethanol and water H-bonding with the solute [31], the latter much stronger. And if we consider the fact that the water content in the alcohols is usually substantial[15] it means that the H-bonding is already established even in ethanol and the observed spectral changes are result of change of the medium as whole.

One additional proof in this respect is the fact that the calculated individual curves on the neutral forms in 10% and in 30% water (Fig. 2a) reproduce well the spectra in Fig. 5b, which confirms our hypothesis for establishment of new solvation equilibrium in mixed DMSO/water solvents.

References

[1] J. Fabian, H. Hartmann, Light Absorption of Organic Colorants, in Reactivity and Structure Concepts in Organic Chemistry, vol. 12, Springer-Verlag, Berlin, 1980.
[2] P.M. Blanchard, A. Gilbert, G.R. Mitchell, J. Mater. Chem. 3 (1993) 1015.
[3] I.Ya. Bershtein, O.F. Ginsburg, Russ. Chem. Rev. 41 (1972) 97.
[4] J.G. Mohr, O.S. Wolfbeis, Anal. Chim. Acta 292 (1994) 41.
[5] T. Stoyanova, S. Stoyanov, L. Antonov, V. Petrova, Dyes Pigm. 31 (1996) 1.
[6] S. Stoyanov, L. Antonov, T. Stoyanova, V. Petrova, Dyes Pigm. 32 (1996) 171.
[7] L. Antonov, D. Nedeltcheva, Chem. Soc. Rev. 29 (2000) 217.
[8] L. Antonov, D. Nedeltcheva, Anal. Lett. 29 (1996) 2055.
[9] L. Antonov, V. Petrov, Anal. Bioanal. Chem. 374 (2002) 1312.
[10] M. Albota, D. Beljionne, J.-L. Bredas, J.E. Ehrlich, J.-Y. Fu, A.A. Heikal, S.E. Hess, T. Kogej, M.D. Levin, S.R. Marder, D. McCord-

[13] In fact specific NH···O═S(Me)$_2$ interactions cannot be excluded.

[14] It is interesting to mention that in the case of **B** and **C** the new solvation equilibrium is already established at 10% water, confirming that the solvation in DMSO is probably less preferred.

[15] In [5,6] 96% spectral grade ethanol has been used.

Maughon, J.W. Perry, H.R. Rumi, G. Subramaniam, W.W. Webb, X.-L. Wu, C. Xu, Science 281 (1998) 1653.
[11] L. Antonov, K. Kamada, K. Ohta, F.S. Kamounah, Phys. Chem. Chem. Phys 5 (2003) 1193.
[12] X.M. Wang, D. Wang, G.Y. Zhou, W.T. Yu, Y.F. Zhou, Q. Fang, M.H. Jiang, J. Mater. Chem. 11 (2001) 1600.
[13] M. Sheik-Bahae, A.A. Said, T.H. Wei, D.J. Hagan, E.W. Vansstryland, IEEE J. Quantum Electron. 26 (1990) 760.
[14] P. Audebert, K. Kamada, K. Matsunaga, K. Ohta, Chem. Phys. Lett. 367 (2003) 62.
[15] L. Antonov, K. Kamada, K. Ohta, Appl. Spectr. 56 (2002) 1508.
[16] M.J. Frisch, G.W. Trucks, H.B. Schlegel, G.E. Scuseria, M.A. Robb, J.R. Cheeseman, V.G. Zakrzewski, J.A. Montgomery Jr., R.E. Stratmann, J.C. Burant, S. Dapprich, J.M. Millam, A.D. Daniels, K.N. Kudin, M.C. Strain, O. Farkas, J. Tomasi, V. Barone, M. Cossi, R. Cammi, B. Mennucci, C. Pomelli, C. Adamo, S. Clifford, J. Ochterski, G.A. Petersson, P.Y. Ayala, Q. Cui, K. Morokuma, D.K. Malick, A.D. Rabuck, K. Raghavachari, J.B. Foresman, J. Cioslowski, J.V. Ortiz, B.B. Stefanov, G. Liu, A. Liashenko, P. Piskorz, I. Komaromi, R. Gomperts, R.L. Martin, D.J. Fox, T. Keith, M.A. Al-Laham, C.Y. Peng, A. Nanayakkara, C. Gonzalez, M. Challacombe, P.M.W. Gill, B. Johnson, W. Chen, M.W. Wong, J.L. Andres, C. Gonzalez, M. Head-Gordon, E.S. Replogle, J.A. Pople, R.A.6. Gaussian 98, Gaussian, Inc., Pittsburgh, PA, 1998.
[17] V. Barone, M. Cossi, J. Tomasi, J. Comput. Chem. 19 (1998) 404.
[18] S. Miertus, E. Scrocco, J. Tomasi, Chem. Phys. 55 (1981) 117.
[19] J.R. Pliega Jr., J.M. Riveros, Phys. Chem. Chem. Phys. 4 (2002) 1622.
[20] J. Kelemen, J. Kormany, G. Rihs, Dyes Pigm. 3 (1982) 249.
[21] P.F. Gordon, P. Gregory, Organic Chemistry in Colour, Springer-Verlag, Berlin, 1983.
[22] H. Mustroph, Dyes Pigm. 15 (1991) 129.
[23] S. Delysse, P. Raimond, J.-M. Nunzi, Chem. Phys. 219 (1997) 341.
[24] J. Catalan, C. Diaz, F. Garcia-Blanco, J. Org. Chem. 66 (2001) 5846.
[25] A.K. Soper, A. Luzar, J. Chem. Phys. 97 (1992) 1320.
[26] A. Bagno, M. Campulla, M. Pirana, G. Scorrano, S. Slitz, Chem. Eur. J. 5 (1999) 1291.
[27] D.N. Shin, J.W. Wijnen, J.B.F.N. Engberts, A. Wakisaka, J. Phys. Chem. B 106 (2002) 6014.
[28] I.I. Vaisman, M.L. Berkowitz, J. Am. Chem. Soc. 114 (1992) 7889.
[29] I.A. Borin, M.S. Skaf, Chem. Phys. Lett. 296 (1998) 125;
I.A. Borin, M.S. Skaf, J. Chem. Phys. 110 (1999) 6412.
[30] B. Kirchner, M. Reiher, J. Am. Chem. Soc. 124 (2002) 6206.
[31] W.R. Brode, I.L. Seldin, P.E. Spoerri, G.M. Wyman, J. Am. Chem. Soc. 77 (1955) 2762.